Diffuse ferroelectric transition and relaxational dipolar freezing in $(Ba, Sr)TiO_3$: II. Role of Sr concentration in the dynamics of freezing

1996 J. Phys.: Condens. Matter 8 4269

(http://iopscience.iop.org/0953-8984/8/23/018)

J. Phys.: Condens. Matter **8** (1996) 4269–4287. Printed in the UK

Diffuse ferroelectric transition and relaxational dipolar freezing in (Ba,Sr)TiO_3: II. Role of Sr concentration in the dynamics of freezing

Neelam Singh and Dhananjai Pandey

School of Materials Science and Technology, Banaras Hindu University, Varanasi 221005, India

Received 8 June 1995, in final form 16 November 1995

Abstract. A distinction between the behaviour of $(Ba_{1-x}Sr_x)TiO_3$ samples with $x \leqslant 0.12$ and $x \geqslant 0.16$ is made on the basis of thermal hysteresis in the temperature dependence of the dielectric constant and the frequency dependence of the temperature at which the dielectric constant peaks. The scaling behaviour of the dielectric loss spectra for all the compositions suggests that the distribution of relaxation times is temperature independent. It is proposed that, for $x \leqslant 0.12$ and $x \geqslant 0.16$, the system is in a domain and dipolar glass state, respectively.

1. Introduction

The last two decades have witnessed [1, 2] extensive interest in incipient ferroelectrics such as $KTaO_3$ and $SrTiO_3$ containing random site dipolar impurities. The random site dipoles result from off-centre positions of impurities like Li and Nb which substitute for K and Ta, respectively, in $KTaO_3$. These random site dipoles carry larger polarization clouds due to the high polarizability of the host matrix. With increasing concentration of the random site dipolar impurities, a percolative type of phase transition into the long-range ordered ferroelectric state can occur [3]. This is a consequence of the indirect dipole–host lattice–dipole interaction due to the high polarizability of the incipient ferroelectric host lattice. Below the percolation threshold, the random local fields (RFs) associated with the random dipoles prevent [4] the appearance of long-range ferroelectric-like order and lead to a dipolar glass state.

The ferroelectric behaviour of materials such as $BaTiO_3$ and $PbTiO_3$ is also known to be influenced by random site impurities at both Ba and Ti sites. One of the consequences [5–7] of these random site impurities is the smearing out of dielectric constant versus temperature plots. In the early literature the term 'diffuse phase transition' was coined for such smeared responses and was attributed to factors such as the inhomogeneous distribution of impurity atoms [8, 9] or grain size effect [10, 11] in ceramic specimens. Recent extensive work on (Ba, Ca)TiO_3 [5, 12] and (Ba, Sr)TiO_3 [6] systems by our group has conclusively established that the smeared-out response in these systems is not due to extrinsic factors such as compositional inhomogeneities and grain size but is intrinsically due to the presence of the random site substitutional impurities. It has been shown that, with increasing concentration of the random site impurity, smearing of the ϵ' versus T plots increases as also does the departure from Curie–Weiss behaviour above the dielectric constant (ϵ') peak temperature T'_m. More recently, it has been shown [6] that $Ba_{0.92}Sr_{0.08}TiO_3$ exhibits relaxational dipolar

0953-8984/96/234269+19$19.50

freezing below the dielectric constant peak temperature T_m'. However, no measurements were carried out on samples containing higher Sr contents in this work. Since the sizes of both Ca and Sr are smaller than that of Ba, it was argued [6] that these impurity atoms may take up off-centre positions, giving rise to local dipoles and random local fields. On account of the strong ferroelectric interactions in the $BaTiO_3$ host matrix and simultaneous presence of quenched random fields, the system may undergo a transition to the so-called 'domain state' [13] which permits [14] ferroelectric order on mesoscopic length scales if the RFs are weak. These RF domains are generally smaller than the usual twin-related transformation domains (e.g. the familiar 90° and 180° domains for the tetragonal phase) in the pure system and may have irregular boundaries [14]. With increasing impurity concentration beyond a certain critical concentration, the RF domains may become too small to be stable against thermal fluctuations. In this situation, the system is expected to behave like a cluster dipole glass [15]. It is interesting to note that the random site dipolar impurities in incipient ferroelectrics stabilize the ferroelectric-like state above a critical concentration while random site dipolar impurities in regular ferroelectrics can lead to its degeneration into a cluster dipolar glass state. Very little work has been done to understand the role of random site impurities in destroying the ferroelectric state of the host lattice.

The present investigation is a continuation of our previous work [6] to understand the effect of Sr substitution on the ferroelectric behaviour of $BaTiO_3$. A series of new experimental observations are presented to show that Sr substitution beyond 12 at.% concentration can lead to dipole-glass-like behaviour whereas for concentrations of 12 at.% or less the situation is ferroelectric like, possibly over mesoscopic length scales. In the present work, we have resolved (i) the difference in the T_m' and T_m'' (ii) the frequency dependence of T_m' and T_m'' and (iii) the thermal hysteresis in the heating and cooling cycles in an unambiguous manner compared with our previous work. In addition, we have looked at the phenomenon of relaxational freezing in this system for four different strontium concentrations compared with only $x = 0.08$ in the previous work. The analysis of the ϵ' and ϵ'' versus $\log f$ data has been performed assuming distribution of relaxation times as confirmed by Cole–Cole plots as well as the scaling behaviour of dielectric loss for all the compositions including that with $x = 0.08$ for which we had assumed the Debye model in our previous work [6].

2. Experimental details

$(Ba, Sr)TiO_3$ powders were prepared using the semiwet (SW) method involving solid state thermochemical reaction between $(Ba, Sr)CO_3$ and TiO_2 particles as described in our previous work [6]. The precursors $(Ba, Sr)CO_3$ were prepared using the chemical coprecipitation technique. Such a SW method yields compositionally homogeneous $(Ba, Sr)TiO_3$ powders as shown earlier [6]. These powders were sintered into ceramic pellets under conditions described in our earlier work. These pellets were about 1.5–2 mm thick and their diameter was around 1.4 mm. The ceramic pellets were electroded with air-dried silver paste which had been cured at 120 °C. The dielectric measurements were carried out using a Schulemberger impedance–gain phase analyser model 1260. The temperature was controlled to within ±1 °C using a programmable temperature controller. The rate of heating for the dielectric measurements involving the temperature dependences of capacitance and $\tan\delta$ at 1, 10 and 100 kHz was optimized as $1^\circ\ \mathrm{min}^{-1}$ which was controlled by the programmable controller. The capacitance and $\tan\delta$ as functions of frequency at selected temperature intervals were recorded in a separate run during cooling from temperatures well above the dielectric constant peak temperature. The rate of cooling in these measurements was also

1 °C min^{-1} with a hold time of 5 min at each temperature. In the earlier study [6], the heating rates during measurements were not programmed; instead, at each temperature the dielectric constant was measured after the temperature had stabilized for 4–5 min. Also the temperature control was inferior in the previous work.

3. Results

3.1. Temperature dependence of dielectric constant

Figures 1, 2, 3 and 4 depict the temperature dependences of the real (ϵ') and imaginary (ϵ'') parts of the dielectric constant at 1, 10 and 100 kHz measured during heating and cooling cycles for $(Ba_{1-x}Sr_x)TiO_3$ samples containing 8 at.% Sr, 12 at.% Sr, 16 at.% Sr and 20 at.% Sr, respectively. The temperatures T'_m corresponding to the peak in the real part of the dielectric constant as obtained in the present work in the heating cycle are nearly the same for all the compositions, except for that with $x = 0.12$ reported in our previous work [6]. In addition, we find that, for $x = 0.08$, the dielectric constant exhibits a reasonably sharp change at T'_m. This sharp change in dielectric constant is gradually replaced by diffuse behaviour where diffuseness increases with increasing strontium concentration. There is a need to distinguish between the temperature dependences of ϵ' and ϵ'' for two different strontium concentration ranges, $x \leqslant 0.12$ and $x > 0.12$, as discussed below.

(i) The temperatures T'_m and T''_m corresponding to the peak in ϵ' and the peak in ϵ'' are coincident within ±1 °C for 8 at.% Sr and 12 at.% Sr concentrations as can be seen from figures 1 and 2. For samples containing 16 at.% Sr and 20 at.% Sr, the two temperatures are not coincident. In particular, $T''_m < T'_m$ for $x > 0.12$ and the difference $T'_m - T''_m$ is a function of measuring frequency. For 1 kHz, these differences are 10 °C and 24 °C for $x = 0.16$ and 0.20, respectively. In materials such as $BaTiO_3$ undergoing the ferroelectric phase transition, the temperatures T'_m and T''_m should be coincident [16] as per the Kramer–Kronig relationship. As discussed by Lines and Glass [17], this difference has to be attributed to temperature-dependent relaxation processes below T'_m. In dipolar [1] as well as spin-glass [18] systems, T''_m is invariably lower than T'_m. In fact, in well known glassy systems [19], the peak in ϵ'' occurs around the inflection point below T'_m in the ϵ' versus T plots. This feature can be seen for samples containing 16 at.% Sr and 20 at.% Sr. All this indicates a gradual transition towards a dipole-glass-type behaviour with increasing strontium concentration.

(ii) The characteristic temperatures T'_m and T''_m shift to higher temperatures with increasing measurement frequency for the $x = 0.16$ and 0.20 samples. The shift in T''_m is more prominent than that in T'_m. No such shifts are observed for $x \leqslant 0.12$ within, of course, the accuracy of our temperature measurement, i.e. ±1°C (see figures 1 and 2). For a regular thermodynamic phase transition, the temperatures T'_m and T''_m are not only coincident but also frequency independent. The frequency dependences of T'_m and T''_m for $x = 0.16$ and 0.20 are similar to what is well known for spin [18] and dipole glasses [1] where T'_m is identified as a freezing temperature T_f. The possibility that the frequency-dependent shifts in T'_m and T''_m for $x \leqslant 0.12$ are within ±1 °C (accuracy of our measurement) seems remote since, for these concentrations, T'_m and T''_m are also coincident as pointed out in (i) above.

(iii) There is one more piece of evidence which suggests the necessity of making a distinction between the temperature-dependent dielectric responses for the compositions with $x \leqslant 0.12$ and $x \geqslant 0.16$. For $x \leqslant 0.12$, the temperature dependences of both the real and the imaginary parts of the dielecric constant show thermal hysteresis in the heating and

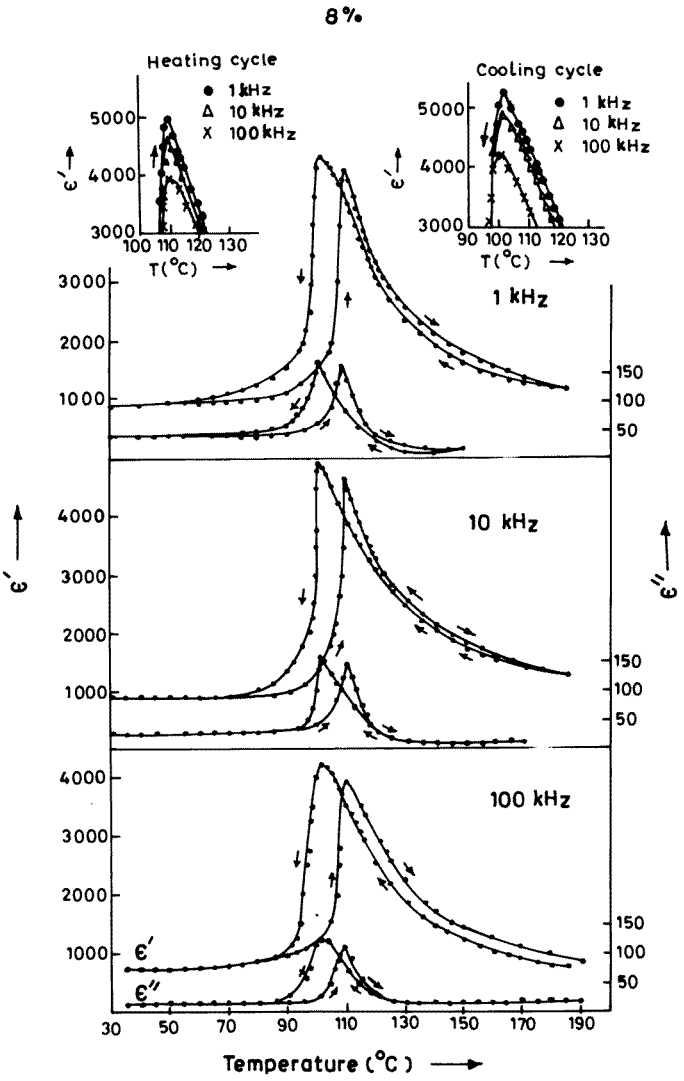

Figure 1. Temperature dependences of ϵ' and ϵ'' at 1, 10 and 100 kHz measured during heating and cooling cycles for $(Ba_{0.92}Sr_{0.08})TiO_3$. The insets at the top depict the effect of frequency on T'_m.

cooling cycles. This is characteristic of any first-order phase transition such as the cubic–tetragonal phase transition in $BaTiO_3$. The only difference in the strontium-substituted samples compared with $BaTiO_3$ is the slight frequency dependence in the temperature of onset of the hysteresis for $x = 0.12$ in the heating cycle. For $x > 0.12$, the nature of thermal hysteresis is completely different in the sense that ϵ'' is anhysteric in the heating and cooling cycles. Also the very small hysteresis for the 16 at.% Sr and 20 at.% Sr samples is not of the type observed in a first-order phase transition. It may be noted that, for pure thermal hysteresis arising out of the phase coexistence region for a first-order phase transition, one expects the heating and cooling curves to be nearly coincident at temperatures above T'_m/T''_m for both the cycles. The fact that this is not so in figures 1 and 2 suggests that the

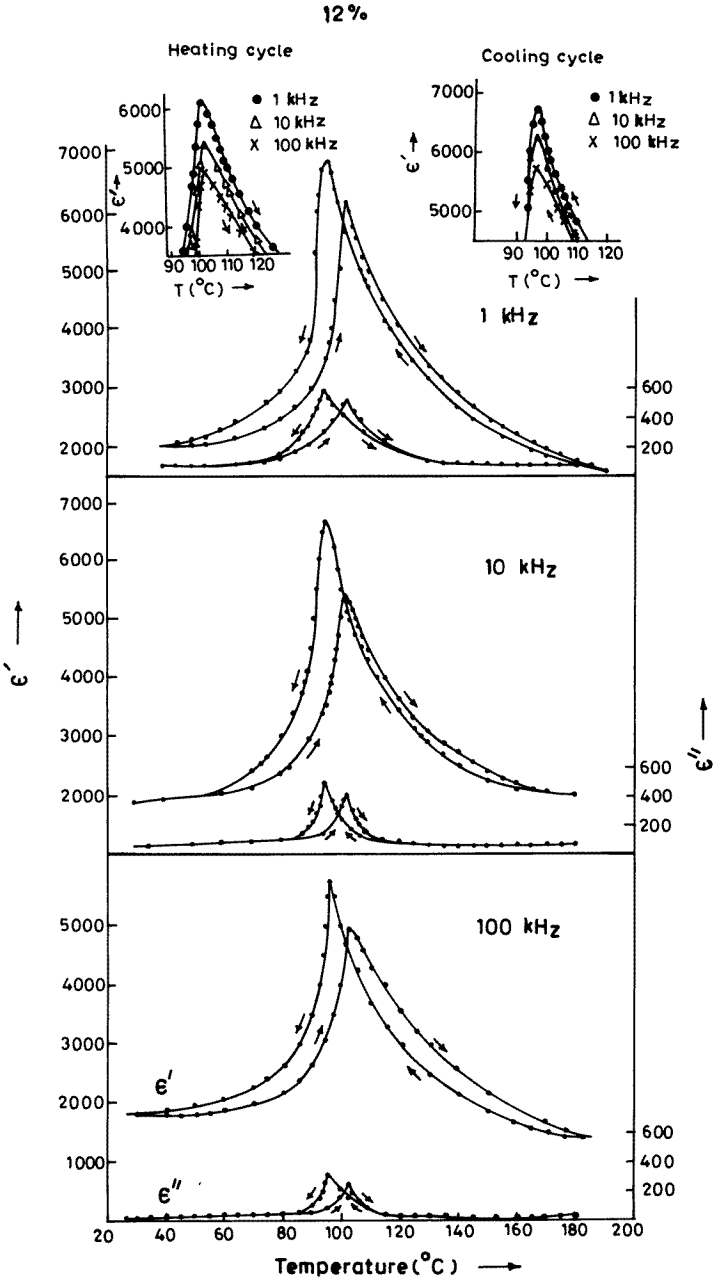

Figure 2. Temperature dependences of ϵ' and ϵ'' at 1, 10 and 100 kHz measured during heating and cooling cycles for $(Ba_{0.88}Sr_{0.12})TiO_3$. The insets at the top depict the effect of frequency on T'_m.

cooling rate should have been a little slower to observe pure thermal hysteresis. However, the hysteresis above T'_m/T''_m is in general smaller than that below T'_m/T''_m, confirming the presence of pure thermal hysteresis in addition to the artefacts of faster cooling.

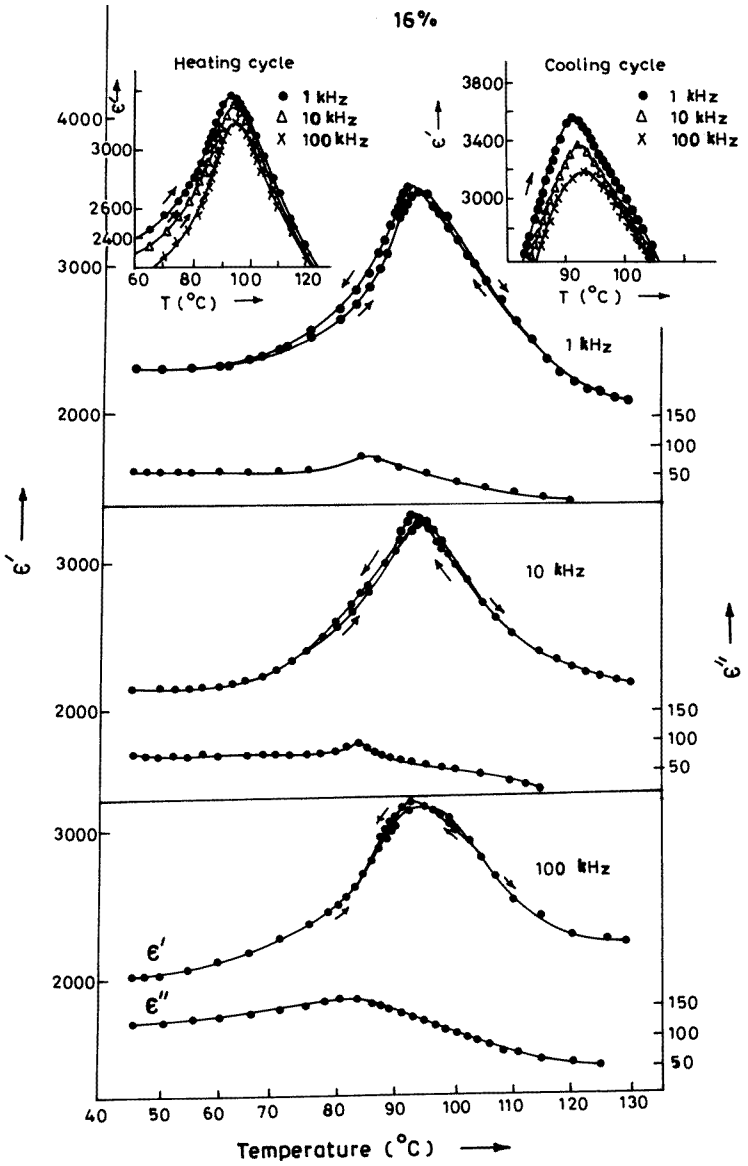

Figure 3. Temperature dependences of ϵ' and ϵ'' at 1, 10 and 100 kHz measured during heating and cooling cycles for $(Ba_{0.84}Sr_{0.16})TiO_3$. The insets at the top depict the effect of frequency on T'_m.

3.2. Relaxational freezing

One of the characteristics of the dipolar glass systems as well as relaxor ferroelectrics such as $Pb(Mg_{1/3}Nb_{2/3})O_3$ (PMN) is the appearance [1, 20–24] of a low-frequency dielectric loss peak below T'_m in the ϵ'' versus log f plots. These loss peaks shift to lower frequencies on decreasing the temperature, indicating the thermally activated nature of dielectric relaxation.

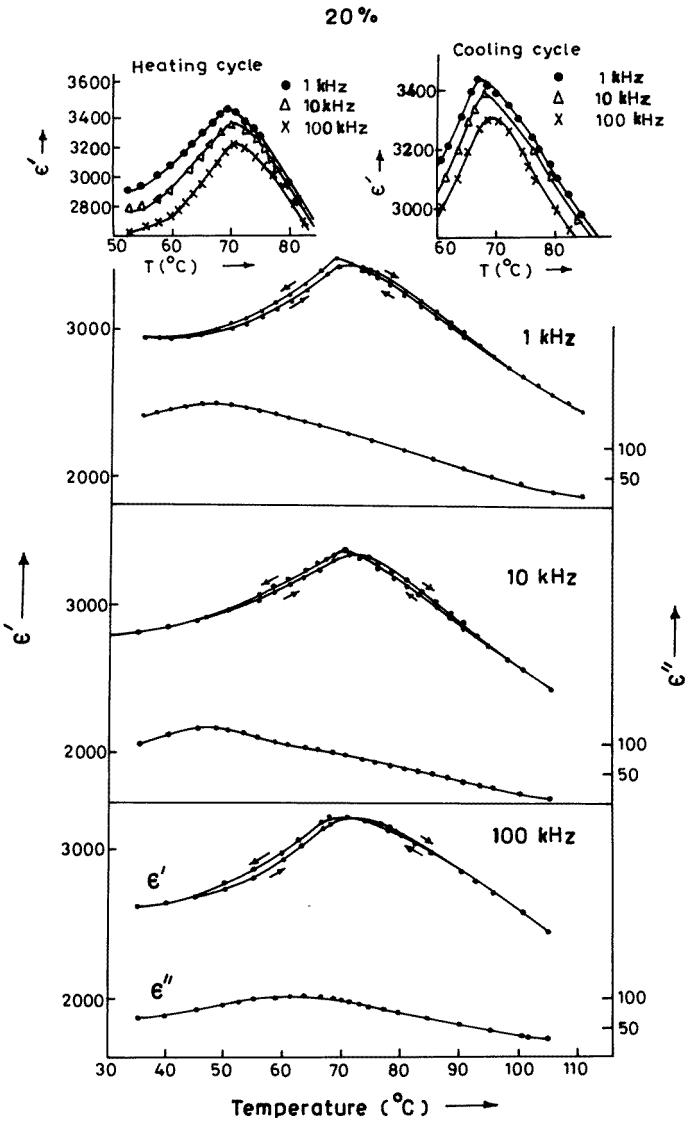

Figure 4. Temperature dependences of ϵ' and ϵ'' at 1, 10 and 100 kHz measured during heating and cooling cycles for $(Ba_{0.8}Sr_{0.2})TiO_3$. The insets at the top depict the effect of frequency on T'_m.

These studies have thrown light on the nature of freezing of dipolar clusters below T'_m. Figures 5, 6, 7 and 8 depict the ϵ'/ϵ'' versus log f plots at various temperatures for $x = 0.08$, 0.12, 0.16 and 0.20, respectively. All these measurements were performed during the cooling cycle. For $x \leqslant 0.16$, these loss peaks appeared below T'_m whereas for $x = 0.20$ the loss peaks appeared above T'_m. In addition, we have found evidence for two loss peaks at 90 °C ($> T'_m$) for $x = 0.20$. With decreasing temperature, the high-frequency peak eventually disappears at around T'_m. As discussed later, the high-frequency peak is most probably due to the lattice relaxation which shows a critical slowing down on approaching T'_m from

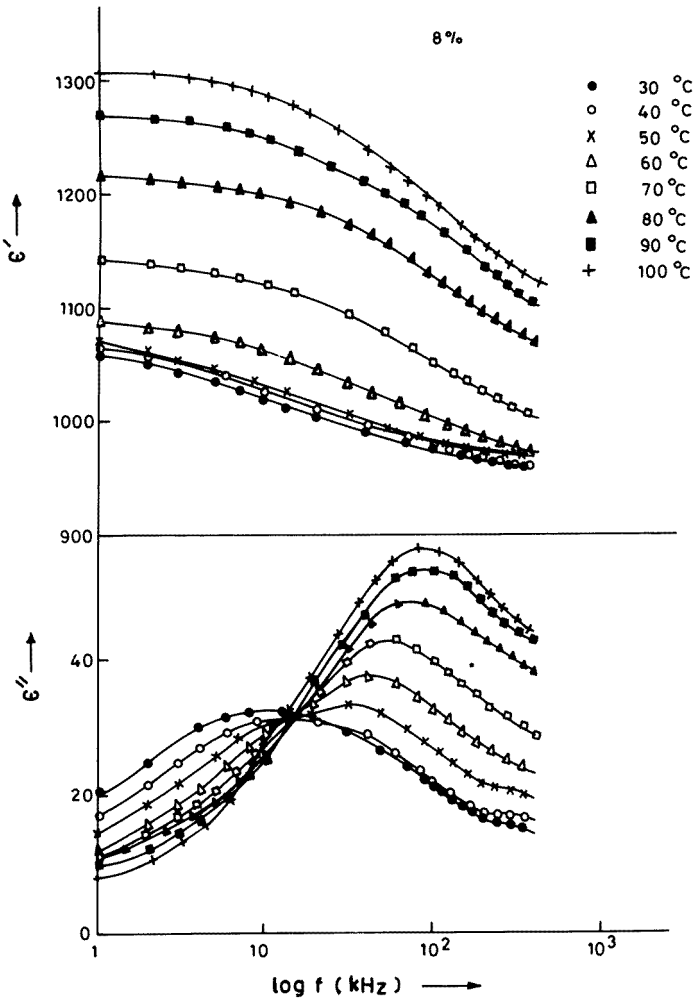

Figure 5. Frequency dependences of ϵ' and ϵ'' at various temperatures for $(Ba_{0.92}Sr_{0.08})TiO_3$.

below as well as above this temperature, as reported for PMN also [22]. Because of the extreme slowing down of lattice relaxation near T'_m, the second peak becomes accessible at frequencies where only dipolar cluster dynamics are normally expected to contribute. As expected, on going well below T'_m, the lattice relaxation process has again become inaccessible for the frequency window of the present investigation.

In our previous work [6], we analysed the data for $x = 0.08$ assuming a monodispersive Debye relation. However, the width of the loss peaks in figures 5–8 cannot be accounted for in terms of a monodispersive relaxation process but points towards the possibility of a distribution of relaxation times. We settle this issue in several ways as discussed below.

3.3. Cole–Cole plots

One of the most convenient ways for checking the polydispersive nature of dielectric relaxation is through complex Argand plane plots between ϵ'' and ϵ', usually called Cole–

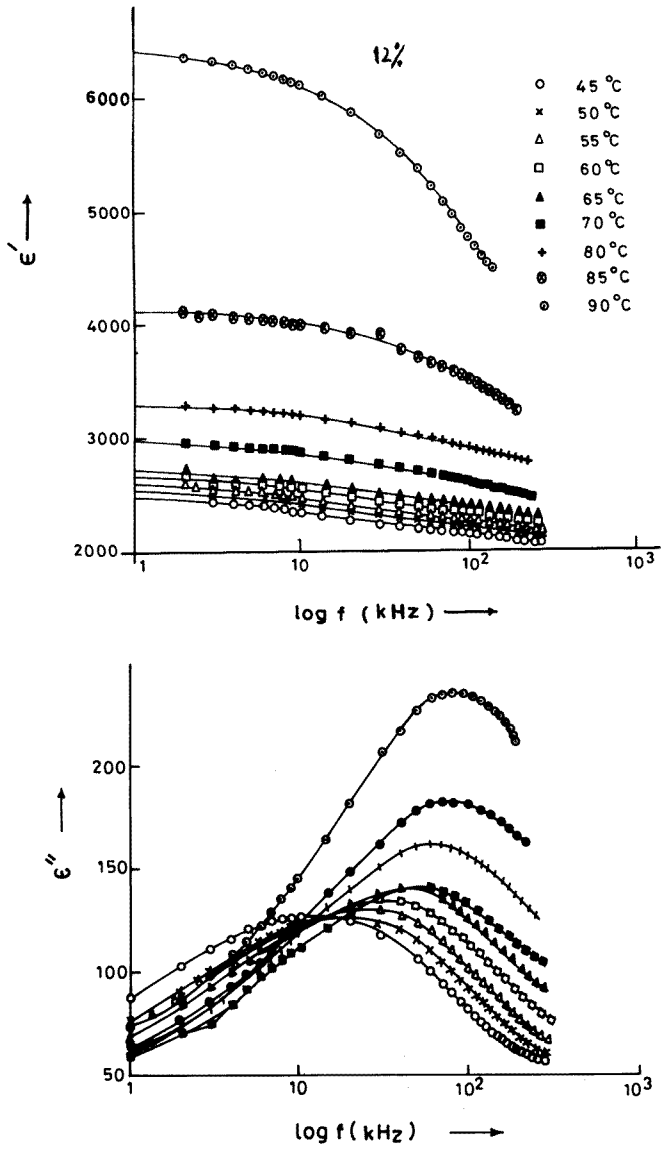

Figure 6. Frequency dependences of ϵ' and ϵ'' at various temperatures for $(Ba_{0.88}Sr_{0.12})TiO_3$.

Cole plots. For a pure monodispersive Debye process, one expects semicircular plots with a centre located on the ϵ' axis whereas, for polydispersive relaxation, these Argand plane plots are close to circular arcs. The complex dielectric constant in such situations is known to be described by the empirical relation $\epsilon^* = \epsilon' - i\epsilon'' = \epsilon_\infty + (\epsilon_s - \epsilon_\infty)/[1 + (i\omega\tau)^{1-\alpha}]$, where ϵ_s and ϵ_∞ are the low- and high-frequency values of ϵ', α is a measure of the distribution of relaxation times, $\tau = \omega^{-1}$ and $\omega = 2\pi f$. The parameter α can be determined from the location of the centre of the Cole–Cole circles of which only an arc lies above the ϵ' axis. Figures 9 and 10 depict two representative plots for $x = 0.12$ and 0.16. It is evident from these figures that the relaxation process differs very significantly from the monodispersive

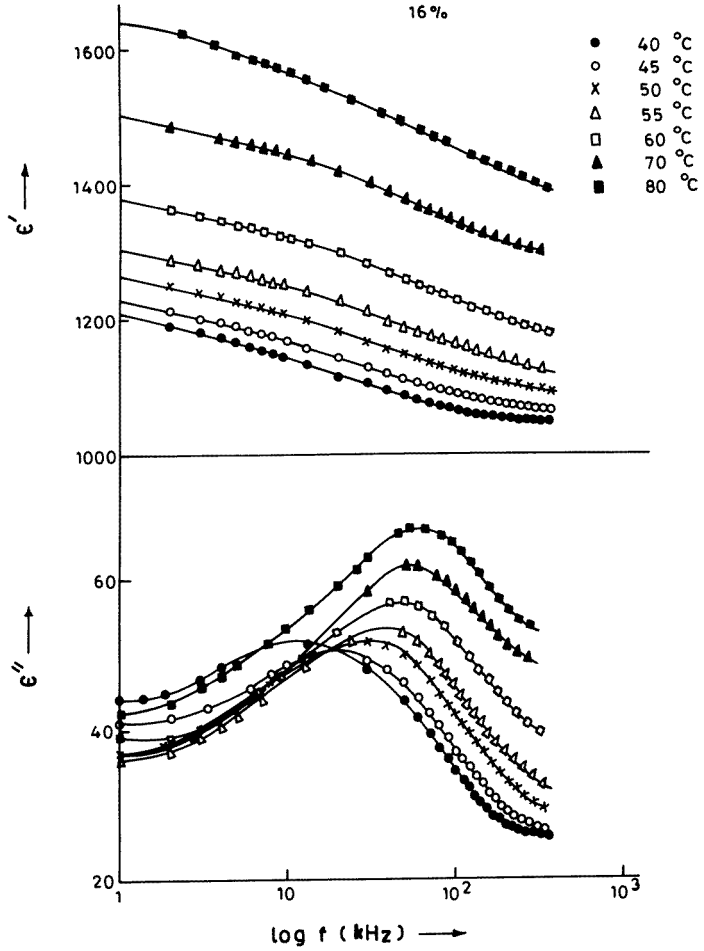

Figure 7. Frequency dependences of ϵ' and ϵ'' at various temperatures for $(Ba_{0.84}Sr_{0.16})TiO_3$.

Debye process (for which $\alpha = 0$) for all compositions and temperatures. The parameter α, as determined from the angle subtended by the radius of the circle with the ϵ' axis passing through the origin of the ϵ'' axis, shows a very small increase in the interval $[0.45, 0.49]$ and $[0.38, 0.45]$ with decreasing temperature for compositions with $x = 0.12$ and 0.16, implying a slight increase in the distribution of the relaxation time with decreasing temperature below T'_m. The flat shape of the Cole–Cole plots just below T'_m on the high-frequency side suggests the overlap of a low-frequency process due to cluster dynamics and a high-frequency process (which is only partly covered in the frequency range of our investigations) due to lattice relaxations to be discussed later.

3.3.1. Scaling behaviour of $\epsilon''(\omega, T)$. The Cole–Cole plots given in the previous section confirm the polydispersive nature of dielectric relaxation for all the compositions. However, the small variation in α with decreasing temperature is not convincing enough, keeping in mind the uncertainties in fitting the circle which was done through a visual fit to the observed data points. We can look at the distribution of relaxation times from yet another angle. If

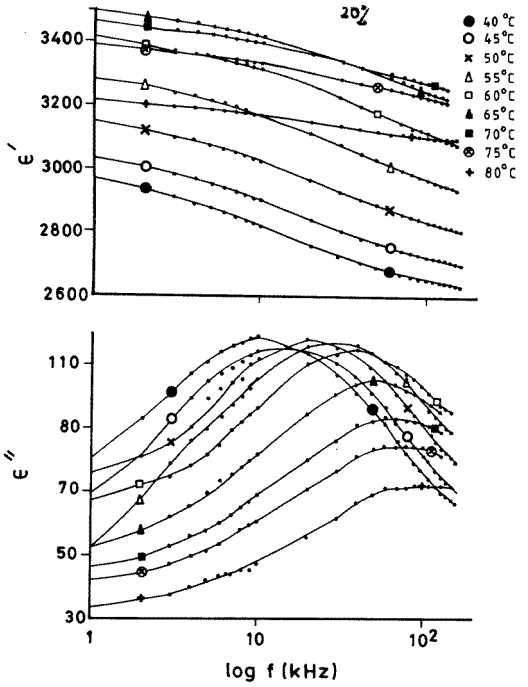

Figure 8. Frequency dependences of ϵ' and ϵ'' at various temperatures for $(Ba_{0.80}Sr_{0.20})TiO_3$.

$g(\tau, T)$ is the temperature-dependent distribution function for relaxation times, the complex dielectric constant can be expressed as [25]

$$\epsilon^* - \epsilon_\infty = \epsilon(0, T) \int \frac{g(\tau, T)\mathrm{d}(\ln \tau)}{1 - \mathrm{i}\omega\tau}$$

where $\epsilon(0, T)$ is the low-frequency dielectric constant. As shown by Courtens [19], for a broad relaxation time distribution function $g(\tau, T)$ in $\ln \tau$, $\epsilon''(\omega, T)$ can be approximated as

$$\epsilon''(\omega, T) \simeq \frac{\pi}{2}\epsilon(0, T)g\left(\frac{1}{\omega}, T\right).$$

If the frequency-independent term $(\pi/2)\epsilon(0, T)$ on the right-hand side is ignored, $\epsilon''(\omega, T)$ directly corresponds to the relaxation time distribution function $g(1/\omega, T)$. If we plot the $\epsilon''(\omega, T)$ data in scaled coordinates, i.e. $\epsilon''(\omega, T)/\epsilon''(\omega_{max}, T)$ and $\log(\omega/\omega_{max})$, where ω_{max} corresponds to the frequency of the loss peak in the ϵ'' versus $\log f$ plots, the entire dielectric loss data can be collapsed into one master curve as shown in figures 11, 12, 13 and 14 for $x = 0.08$, 0.12, 0.16 and 0.20, respectively. The collapse of the entire $\epsilon''(\omega, T)$ data into a single master curve is better for strontium concentrations $x = 0.16$ and 0.20 than for $x = 0.08$ and 0.12. The scaling behaviour of $\epsilon''(\omega, T)$ clearly indicates that the distribution function for relaxation times is nearly temperature independent and thus not much significance can be attached to the small variation in the Cole–Cole plot variable α with decreasing temperature. A similar collapse of the $\epsilon''(\omega, T)$ data onto one single master curve has been demonstrated by Colla *et al* [21] for PMN in the temperature range 185 K $< T <$ 260 K.

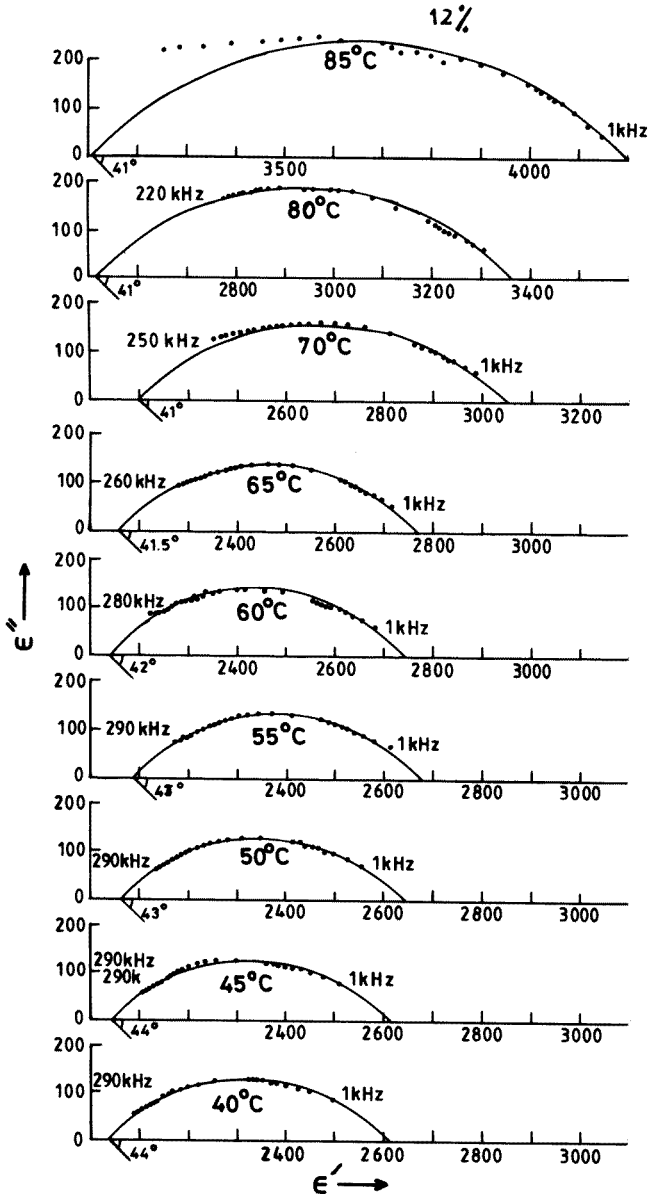

Figure 9. Cole–Cole plots at various temperatures for $(Ba_{0.88}Sr_{0.12})TiO_3$.

3.3.2. Temperature dependence of the most probable relaxation time. In our previous work [6], we determined the relaxation time τ as a function of temperature for $x = 0.08$ using the monodispersive Debye equation. It is, however, evident from the Cole–Cole plots as well as the relaxation time distribution function $g(1/\omega, T)$ that the use of monodispersive Debye equations is not justified even for $x = 0.08$. In such a situation, instead of determining τ using the equation [6] $\epsilon' = \epsilon_s - \omega\tau\epsilon''$ for monodispersive relaxation, one should determine the most probable relaxation time τ_m from the position of the loss peak in the ϵ'' versus

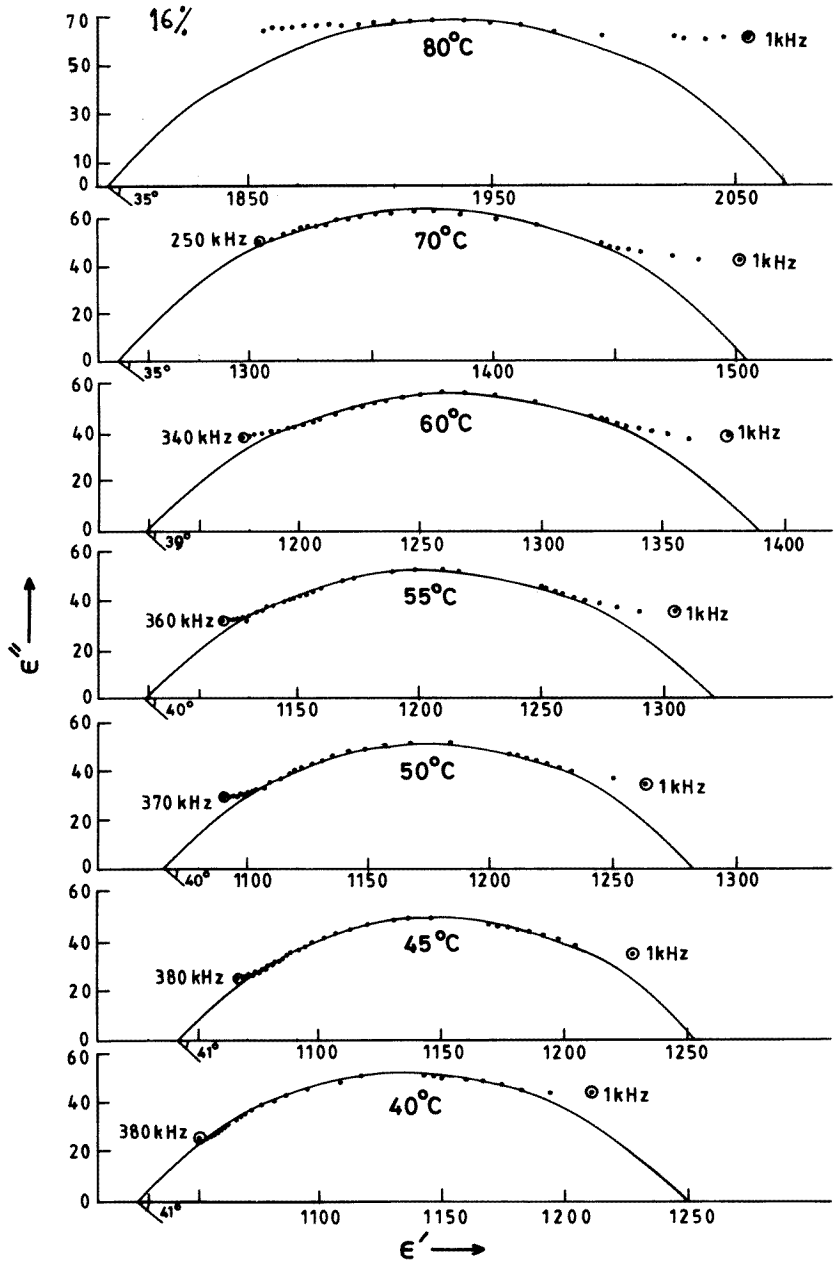

Figure 10. Cole–Cole plots at various temperatures for $(Ba_{0.84}Sr_{0.16})TiO_3$.

log f plots.

The most probable relaxation time follows an Arrhenius-type temperature dependence below T_m' for all the compositions as can be seen from the straight-line fits to the $\ln\tau$ versus $1/T$ plots in figure 15. For $x = 0.20$, the $\ln\tau$ versus $1/T$ plot clearly suggests two different slopes for relaxation processes above and below T_m'. As pointed out earlier, and to be discussed in detail later, the determination of τ_m from the peak position of the ϵ''

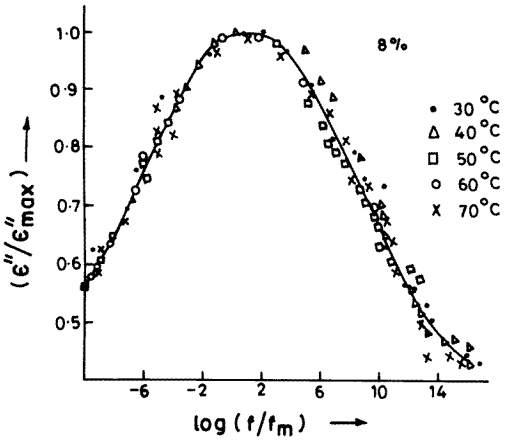

Figure 11. Scaling behaviour of ϵ'' data at various temperatures for $(Ba_{0.92}Sr_{0.08})TiO_3$.

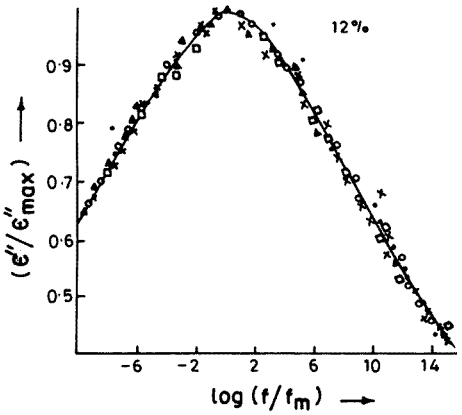

Figure 12. Scaling behaviour of ϵ'' data at various temperatures for $(Ba_{0.88}Sr_{0.12})TiO_3$.

versus log f plot above 60 °C for $x = 0.20$ becomes unreliable due to the overlap between the cluster relaxation process and the lattice relaxations in the vicinity of T'_m because of the critical slowing down of the lattice relaxation process. The two relaxation processes are not resolved until the temperature approaches 90 °C. There is, however, no ambiguity in the determination of τ_m from the low-frequency peak for $T \leqslant 60$ °C. Notwithstanding these problems for $x = 0.20$, the most probable relaxation rate for all the compositions exhibits Arrhenius-type temperature dependence below T'_m. The activation energies ΔE determined from these plots are 0.34, 0.40, 0.49 and 0.62 eV for $x = 0.08$, 0.12, 0.16 and 0.20, respectively. Thus the activation energy increases with increasing strontium concentration. The inverse of the attempt frequency τ_0 seems to be the highest for $x = 0.08$ (3.2×10^{-11} s) but remains almost the same for $0.8 < \times \leqslant 0.20$ (4.08×10^{-12}, 2.13×10^{-12} and 4.32×10^{-12} s for $x = 0.12$, 0.16 and 0.20, respectively). The variations in ΔE and τ_0 with Sr concentration are shown in figure 16.

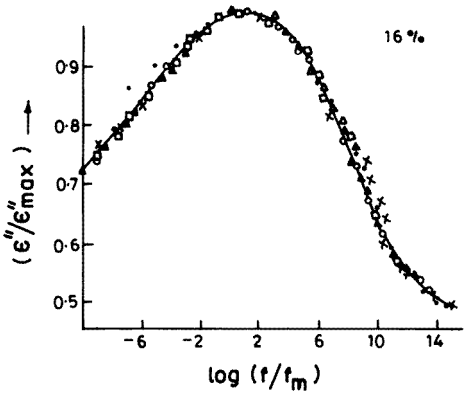

Figure 13. Scaling behaviour of ϵ'' data at various temperatures for $(Ba_{0.84}Sr_{0.16})TiO_3$.

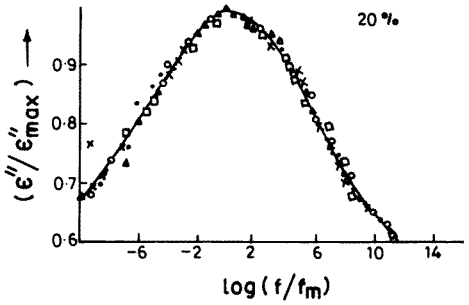

Figure 14. Scaling behaviour of ϵ'' data at various temperatures for $(Ba_{0.80}Sr_{0.20})TiO_3$.

4. Discussion

It is evident from the foregoing that the dielectric behaviours of $(Ba_{1-x}Sr_x)TiO_3$ samples with $x \leqslant 0.12$ and $x \geqslant 0.16$ need to be distinguished. Samples wtih $x \leqslant 0.12$ have several similarities with dielectric anomalies in the pure system ($BaTiO_3$) such as thermal hysteresis, coincidence of T_m' and T_m'', and frequency independence of T_m' and T_m''. On the other hand, the diffuseness of the transition for $x = 0.12$, the departure from Curie–Weiss behaviour over a wider temperature range and the observation of polydispersive low-frequency dielectric loss peaks below T_m' showing Arrhenius-type temperature dependence for the most probable relaxation time distinguish even these two compositions from pure $BaTiO_3$. For samples with $x \geqslant 0.16$, not only does the thermal hysteresis disappear but also T_m' and T_m'' become frequency dependent with T_m'' invariably being lower than T_m'. The Curie–Weiss behaviour is observed at much higher temperatures above T_m' and there is also evidence for Arrhenius-type relaxational freezing below T_m'. All these observations clearly suggest that, with increasing strontium concentration, the system moves away from a regular ferroelectric to a full-blown dipolar glass state. The compositions with $x \leqslant 0.12$ correspond to the transitional state between the two extremes and, as such, possess some of the characteristics of both the dipolar glass state and the ferroelectric state. A similar gradual change in the nature of dielectric anomaly has been reported [26] in $(Pb_{1-x}La_x)(Zr_{0.30}Ti_{0.70})O_{3+x}$ ceramics. For $x < 16$ at.% La, this system exhibits a sharp first-order

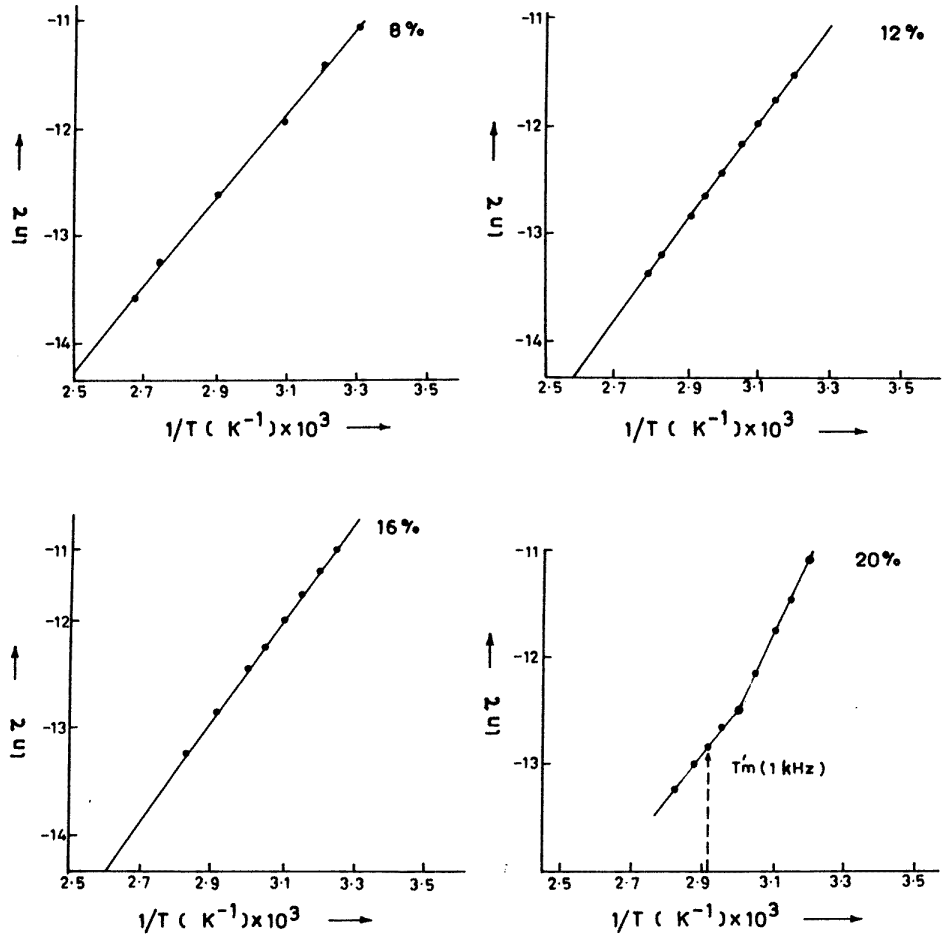

Figure 15. Arrhenius plots for the most probable relaxation time τ_m for $x = 0.08$, 0.12, 0.16 and 0.20.

dielectric anomaly with typical hysteresis and frequency-independent T_m' and T_m'' which are also coincident. For $x > 20$ at.% La, on the other hand, the thermal hysteresis disappears while the temperature variations in ϵ' and ϵ'' become diffuse with $T_m'' < T_m'$, both being frequency dependent also.

It was suggested in our previous work [6] that strontium substitution may give rise to RFs in $BaTiO_3$ due to a possible off-centre occupancy of strontium ions because their ionic radius is smaller than that of the barium ions in a way similar to what is now well known for Li- and Na-substituted $KTaO_3$ [1] or Ca-substituted $SrTiO_3$ [27, 28]. We feel that such RFs may lead the system for smaller strontium concentrations ($x \leqslant 0.12$) to a domain state [29] where ferroelectric-like behaviour can exist over mesoscopic length scales only. The low-frequency polydispersive dielectric relaxations in the ϵ'/ϵ'' versus $\log f$ plots and the rounding of the ϵ' versus T plot for $x = 0.12$ may then be associated with the mesoscopic domain structure below T_m' similar to that reported [28] for $(Sr, Ca)TiO_3$. With increasing strontium concentration beyond $x = 0.12$, the RF domains become too small to stabilize the

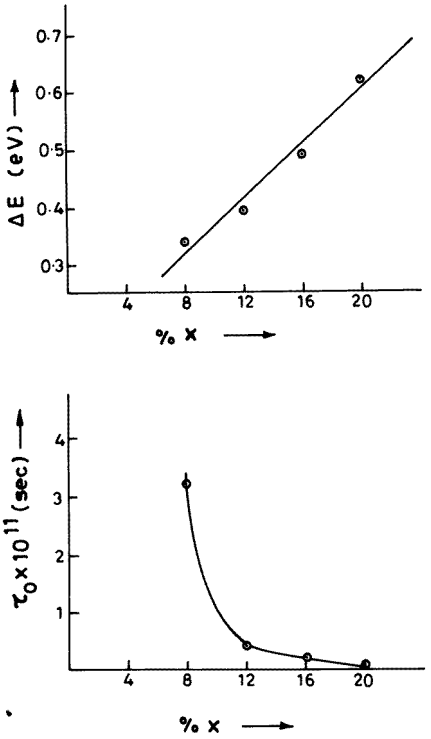

Figure 16. Variations in activation energy and inverse of attempt frequency with Sr concentration.

ferroelectric order even over mesoscopic length scales against thermal fluctuations. Perhaps the destabilization of the RF domains for $x > 0.12$ together with frustrated inter-domain interactions lead to the frequency dependences of T_m' and T_m''. In this description, T_m' for $x \geqslant 0.16$ is actually the freezing temperature linked with the dipolar glass state, albeit the cluster dipolar glass state.

Although we feel that the RFs generated by off-centre strontium ions in the $BaTiO_3$ matrix or off-valent La substitution in $Pb(Zr_{0.3}Ti_{0.7})O_3$ may be responsible for the dipolar glass behaviour in these systems, the random interactions and frustration [30] introduced by strontium and lanthanum substitutions, even though they do not give rise to random site dipoles, may be sufficient to give rise to dipolar glass behaviour above a certain critical concentration. Our main argument in favour of the RF domains is the room-temperature x-ray evidence [6] for ferroelectric symmetry breaking for all the compositions, although the tetragonality decreases with increasing strontium concentration. It will be interesting to examine in future the dynamics of freezing in compositions ($x > 0.20$) where the tetragonality is not discernible at the XRD level.

In the dielectric dispersion of (Ba, Sr)TiO_3, there is a need to distinguish between two different relaxation phenomena: (i) the high-frequency intra-cluster relaxations which we shall call lattice relaxation since it is present even in the host $BaTiO_3$ [31] and (ii) the low-frequency inter-cluster relaxations. Dielectric dispersion in $BaTiO_3$ single crystals as well as ceramics has been observed [31] in the microwave region (10^6–10^9 Hz) in the vicinity of the phase transition temperature. In particular, critical slowing down of the relaxation

time, associated with the hopping of off-centre Ti^{4+} ions in the eight-site potential after the crossover from displacive to order–disorder behaviour, has been verified. This critical relaxation is due to the lattice polarization and has been observed in several order–disorder ferroelectrics such as $NaNO_2$ [32]. Even in materials such as PMN [22] and $(Ba, Sr)TiO_3$ [31], which do not exhibit sharp dielectric anomalies, this high-frequency lattice relaxation in the microwave region has been observed. The relaxation process in these systems also exhibits critical behaviour in the vicinity of the dielectric constant peak temperature T'_m even though it is less critical than that for $BaTiO_3$. These observations have to be attributed to the ferroelectric symmetry breaking over the length scale of clusters within which the dipolar correlations exist. However, unlike $BaTiO_3$, the symmetry breaking in these systems with smeared-out dielectric response is not global below T'_m since the dipolar clusters exhibit a low-frequency relaxational freezing below a frequency-dependent dielectric peak temperature T'_m. Arrhenius-type analysis of the temperature-dependent relaxation time τ, as determined from the frequency-dependent T'_m, is known to give physically unrealistic values for activation energy ΔE and attempt frequency τ_0^{-1} in spin glasses [18] as well as relaxors such as PMN [9]. A Vogel–Fulcher-type temperature dependence for τ has been proposed in these situations to resolve this anomaly [19, 20, 33]. In PMN, Viehland *et al* [20] have proposed that the width of relaxation time distribution increases with decreasing temperature and becomes essentially flat below a Vogel–Fulcher freezing temperature T_{VF} which is more than 50 °C lower than T'_m. In $(Ba, Sr)TiO_3$, the scaling behaviour of $\epsilon''(\omega, T)$ data from room temperature onwards suggests that, although the relaxation time distribution is broad, it is nearly temperature independent from T'_m right up to room temperature. Since room temperature is considerably lower than T'_m, the possibility of existence of a Vogel–Fulcher freezing temperature in this system is remote although low-temperature measurements are required to settle the issue unambiguously. Even at higher temperatures near T'_m, the characteristic relaxation time in PMN has been found to exhibit non-Arrhenius behaviour. This is, however, due to the overlap of two different relaxation processes associated with the lattice polarization and the cluster dynamics in the vicinity of T'_m, as has been clearly shown by Elissalde *et al* [22] for PMN. The overlapping relaxation processes make the determination of the characteristic relaxation time unreliable near T'_m as pointed out in section 3.3.2 for $(Ba, Sr)TiO_3$ with $x = 0.20$. It is obvious that, due to extreme slowing down of the lattice polarization process on either side of T'_m with a maximum in τ at T'_m, the lattice polarization processes enter into the experimental frequency window over a narrow temperature range near T'_m with characteristic relaxation times becoming comparable with those associated with the freezing of dipolar clusters below T'_m. Christen *et al* [24] prefer to call the two relaxation processes α and β type in analogy to what is known in several other glassy systems [34]. However, in these glassy systems, both processes continuously slow down and disappear from the experimental frequency window one by one. In PMN and $(Ba, Sr)TiO_3$, the slowing down of the high-frequency relaxation process in the vicinity of T'_m shows a somewhat critical behaviour [22, 31] and as such cannot be compared with α relaxation processes in other glassy systems. It is in this respect that PMN and $(Ba, Sr)TiO_3$ may not be canonical dipole glasses [2] but exhibit the characteristic of cluster-dipole glasses.

Acknowledgment

This work was partially supported by the Inter-University Consortium for DAE facilities.

References

[1] Höchli U T, Knorr K and Loidl A 1990 *Adv. Phys.* **39** 405
[2] Vugmeister B E and Glinchuk M D 1990 *Rev. Mod. Phys.* **62** 993
[3] Rod S and Van der Klink J J 1994 *Phys. Rev.* B **49** 15 470
[4] Kleeman W and Klössner A 1993 *Ferroelectrics* **150** 35
[5] Tiwari V S and Pandey D 1994 *J. Am. Ceram. Soc.* **77** 1819
[6] Tiwari V S, Singh Neelam and Pandey D 1995 *J. Phys.: Condens. Matter* **7** 1441
[7] Schmidt G 1990 *Phase Trans.* **20** 127
[8] Smolenskii G A 1970 *J. Phys. Soc. Japan Suppl.* **28** (Supplement) 26
[9] Kirillov V V and Isupov V A 1973 *Ferroelectrics* **5** 3
[10] Bell A J 1993 *Ferroelectr. Lett.* **15** 133
[11] Pandey D, Singh Neelam and Mishra S K 1994 *Indian J. Pure Appl. Phys.* **32** 616
[12] Tiwari V S, Singh Neelam and Pandey D 1994 *J. Am. Ceram. Soc.* **77** 1813
[13] Imry Y and Ma S K 1975 *Phys. Rev. Lett.* **35** 1399
[14] Nattermann T 1990 *Ferroelectrics* **104** 171
[15] Sommer D, Kleemann W and Rytz D 1990 *Ferroelectrics* **106** 137
[16] Jona F and Shirane G 1962 *Ferroelectric Crystals* (London: Pergamon)
[17] Lines M E and Glass A M 1977 *Principles and Applications of Ferroelectrics and Related Materials* (Oxford: Clarendon)
[18] Binder K and Young A P 1986 *Rev. Mod. Phys.* **58** 801
[19] Courtens E 1984 *Phys. Rev. Lett.* **52** 69
[20] Viehland D, Jang S, Cross L E and Wutting M 1991 *Phil. Mag.* B **64** 335
[21] Colla E V, Yu Koroleva E, Okuneva N M and Vakhrushev S B 1992 *J. Phys.: Condens. Matter* **4** 3671
[22] Elissalde C, Ravez J and Gaucher P 1992 *Mater. Sci. Eng.* B **13** 327
[23] Yushin N K and Dorogovtsev S N 1993 *Ferroelectrics* **143** 49
[24] Christen H M, Sommer R, Yushin N K and Van der Klink J J 1994 *J. Phys.: Condens. Matter* **6** 2631
[25] Wagner K W 1913 *Ann. Phys., Lpz.* **40** 817
[26] Stenger C G F and Burggraaf A J 1980 *J. Phys. Chem. Solids* **41** 17
[27] Bednorz J G and Müller K A 1984 *Phys. Rev. Lett.* **52** 2289
[28] Kleemann W and Schremmer H 1989 *Phys. Rev.* B **40** 7428
[29] Kleemann W and Klossner A 1993 *Ferroelectrics* **150** 35
[30] See for example Toulouse J 1994 *Ferroelectrics* **151** 215
[31] Kazaoni S, Ravez J, Elissalde C and Maglione M 1992 *Ferroelectrics* **135** 85
[32] Blinc R and Zeks B 1974 *Soft Modes in Ferroelectrics and Antiferroelectrics* (Amsterdam: North-Holland)
[33] Viehland D, Wutting S and Cross L E 1990 *J. Appl. Phys.* **68** 2916
[34] Johari G 1987 *Molecular Dynamics and Relaxation Phenomena in Glasses (Lect. Notes Phys. 277)* (Berlin: Springer)